

# Low-loss light transmission in a rectangular-shaped hybrid metal trench at 1550 nm

Pengfei Yang,<sup>1</sup> Zhigang Di,<sup>2</sup> and Hongxing Xu<sup>1,3,4,\*</sup>

<sup>1</sup> Beijing National Laboratory for Condensed Matter Physics and Institute of Physics, Chinese Academy of Sciences, Beijing 100190, China

<sup>2</sup> College of Electrical Engineering, Hebei United University, Hebei Tangshan 063009, China

<sup>3</sup> School of Physics and Technology, Wuhan University, Wuhan 430072, China

<sup>4</sup> Division of Solid State Physics/The Nanometer Structure Consortium, Lund University, Box 118, SE-22100 Lund, Sweden

\*[hxxu@iphy.ac.cn](mailto:hxxu@iphy.ac.cn)

**Abstract:** A hybrid plasmonic waveguide consisting of a high-index dielectric core embedded inside a rectangular-shaped metallic trench is proposed and its guiding properties are investigated at the wavelength of 1550 nm. Numerical simulations based on the finite element method have demonstrated that the introduced dielectric core could greatly reduce the modal loss of the metal trench while maintaining strong confinement of light. The effects of dielectric core size, material of the cladding and the dielectric core on the modal properties have been systematically investigated. The proposed hybrid plasmonic structure can be realized employing fabrication techniques of the traditional metal trench waveguides and could be leveraged as important elements for highly-integrated photonic circuits.

©2013 Optical Society of America

**OCIS codes:** (240.6680) Surface plasmons; (130.2790) Guided waves; (230.7370) Waveguides; (250.5300) Photonic integrated circuits.

---

## References and links

1. R. Kirchain and L. Kimerling, "A roadmap for nanophotonics," *Nat. Photonics* **1**(6), 303–305 (2007).
2. D. K. Gramotnev and S. I. Bozhevolnyi, "Plasmonics beyond the diffraction limit," *Nat. Photonics* **4**(2), 83–91 (2010).
3. J. Takahara, S. Yamagishi, H. Taki, A. Morimoto, and T. Kobayashi, "Guiding of a one-dimensional optical beam with nanometer diameter," *Opt. Lett.* **22**(7), 475–477 (1997).
4. P. Berini, "Plasmon-polariton waves guided by thin lossy metal films of finite width: Bound modes of symmetric structures," *Phys. Rev. B* **61**(15), 10484–10503 (2000).
5. D. F. P. Pile, T. Ogawa, D. K. Gramotnev, Y. Matsuzaki, K. C. Vernon, K. Yamaguchi, T. Okamoto, M. Haraguchi, and M. Fukui, "Two-dimensionally localized modes of a nanoscale gap plasmon waveguide," *Appl. Phys. Lett.* **87**(26), 261114 (2005).
6. S. I. Bozhevolnyi, V. S. Volkov, E. Devaux, and T. W. Ebbesen, "Channel plasmon-polariton guiding by subwavelength metal grooves," *Phys. Rev. Lett.* **95**(4), 046802 (2005).
7. S. I. Bozhevolnyi, "Effective-index modeling of channel plasmon polaritons," *Opt. Express* **14**(20), 9467–9476 (2006).
8. E. Moreno, S. G. Rodrigo, S. I. Bozhevolnyi, L. Martín-Moreno, and F. J. García-Vidal, "Guiding and focusing of electromagnetic fields with wedge plasmon polaritons," *Phys. Rev. Lett.* **100**(2), 023901 (2008).
9. R. F. Oulton, V. J. Sorger, D. A. Genov, D. F. P. Pile, and X. Zhang, "A hybrid plasmonic waveguide for subwavelength confinement and long-range propagation," *Nat. Photonics* **2**(8), 496–500 (2008).
10. R. F. Oulton, V. J. Sorger, T. Zentgraf, R. M. Ma, C. Gladden, L. Dai, G. Bartal, and X. Zhang, "Plasmon lasers at deep subwavelength scale," *Nature* **461**(7264), 629–632 (2009).
11. M. Wu, Z. H. Han, and V. Van, "Conductor-gap-silicon plasmonic waveguides and passive components at subwavelength scale," *Opt. Express* **18**(11), 11728–11736 (2010).
12. X. Y. Zhang, A. Hu, J. Z. Wen, T. Zhang, X. J. Xue, Y. Zhou, and W. W. Duley, "Numerical analysis of deep sub-wavelength integrated plasmonic devices based on Semiconductor-Insulator-Metal strip waveguides," *Opt. Express* **18**(18), 18945–18959 (2010).
13. X. He, L. Yang, and T. Yang, "Optical nanofocusing by tapering coupled photonic-plasmonic waveguides," *Opt. Express* **19**(14), 12865–12872 (2011).
14. X. Guo, M. Qiu, J. Bao, B. J. Wiley, Q. Yang, X. Zhang, Y. Ma, H. Yu, and L. Tong, "Direct coupling of plasmonic and photonic nanowires for hybrid nanophotonic components and circuits," *Nano Lett.* **9**(12), 4515–4519 (2009).

15. S. Y. Zhu, T. Y. Liow, G. Q. Lo, and D. L. Kwong, "Fully complementary metal-oxide-semiconductor compatible nanoplasmonic slot waveguides for silicon electronic photonic integrated circuits," *Appl. Phys. Lett.* **98**(2), 021107 (2011).
16. D. X. Dai and S. L. He, "A silicon-based hybrid plasmonic waveguide with a metal cap for a nano-scale light confinement," *Opt. Express* **17**(19), 16646–16653 (2009).
17. Y. S. Bian, Z. Zheng, X. Zhao, J. S. Zhu, and T. Zhou, "Symmetric hybrid surface plasmon polariton waveguides for 3D photonic integration," *Opt. Express* **17**(23), 21320–21325 (2009).
18. I. Avrutsky, R. Soref, and W. Buchwald, "Sub-wavelength plasmonic modes in a conductor-gap-dielectric system with a nanoscale gap," *Opt. Express* **18**(1), 348–363 (2010).
19. M. Z. Alam, J. Meier, J. S. Aitchison, and M. Mojtahedi, "Propagation characteristics of hybrid modes supported by metal-low-high index waveguides and bends," *Opt. Express* **18**(12), 12971–12979 (2010).
20. L. Chen, X. Li, G. P. Wang, W. Li, S. H. Chen, L. Xiao, and D. S. Gao, "A Silicon-Based 3-D Hybrid Long-Range Plasmonic Waveguide for Nanophotonic Integration," *J. Lightwave Technol.* **30**(1), 163–168 (2012).
21. Y. S. Bian, Z. Zheng, Y. Liu, J. S. Zhu, and T. Zhou, "Dielectric-loaded surface plasmon polariton waveguide with a holey ridge for propagation-loss reduction and subwavelength mode confinement," *Opt. Express* **18**(23), 23756–23762 (2010).
22. C.-L. Zou, F.-W. Sun, C.-H. Dong, Y.-F. Xiao, X.-F. Ren, L. Lv, X.-D. Chen, J.-M. Cui, Z.-F. Han, and G.-C. Guo, "Movable Fiber-Integrated Hybrid Plasmonic Waveguide on Metal Film," *IEEE Photon. Technol. Lett.* **24**(6), 434–436 (2012).
23. Y. S. Bian, Z. Zheng, X. Zhao, L. Liu, Y. L. Su, J. S. Liu, J. S. Zhu, and T. Zhou, "Dielectrics Covered Metal Nanowires and Nanotubes for Low-Loss Guiding of Subwavelength Plasmonic Modes," *J. Lightwave Technol.* **31**(12), 1973–1979 (2013).
24. H. Benisty and M. Besbes, "Plasmonic inverse rib waveguiding for tight confinement and smooth interface definition," *J. Appl. Phys.* **108**(6), 063108 (2010).
25. D. Chen, "Cylindrical hybrid plasmonic waveguide for subwavelength confinement of light," *Appl. Opt.* **49**(36), 6868–6871 (2010).
26. Y. S. Zhao and L. Zhu, "Coaxial hybrid plasmonic nanowire waveguides," *J. Opt. Soc. Am. B* **27**(6), 1260–1265 (2010).
27. Y. S. Bian, Z. Zheng, X. Zhao, Y. L. Su, L. Liu, J. S. Liu, J. S. Zhu, and T. Zhou, "Guiding of long-range hybrid plasmon polariton in a coupled nanowire array at deep-subwavelength scale," *IEEE Photon. Technol. Lett.* **24**(15), 1279–1281 (2012).
28. J. T. Kim, "CMOS-Compatible Hybrid Plasmonic Waveguide for Subwavelength Light Confinement and On-Chip Integration," *IEEE Photon. Technol. Lett.* **23**(4), 206–208 (2011).
29. M. S. Kwon, "Metal-insulator-silicon-insulator-metal waveguides compatible with standard CMOS technology," *Opt. Express* **19**(9), 8379–8393 (2011).
30. X. Zuo and Z. Sun, "Low-loss plasmonic hybrid optical ridge waveguide on silicon-on-insulator substrate," *Opt. Lett.* **36**(15), 2946–2948 (2011).
31. Y. S. Bian, Z. Zheng, X. Zhao, Y. L. Su, L. Liu, J. S. Liu, J. S. Zhu, and T. Zhou, "Highly Confined Hybrid Plasmonic Modes Guided by Nanowire-embedded-metal Grooves for Low-loss Propagation at 1550nm," *IEEE J. Sel. Top. Quantum Electron.* **19**(3), 4800106 (2013).
32. Y. S. Bian, Z. Zheng, Y. Liu, J. S. Liu, J. S. Zhu, and T. Zhou, "Hybrid wedge plasmon polariton waveguide with good fabrication-error-tolerance for ultra-deep-subwavelength mode confinement," *Opt. Express* **19**(23), 22417–22422 (2011).
33. J. Zhang, L. K. Cai, W. L. Bai, Y. Xu, and G. F. Song, "Hybrid plasmonic waveguide with gain medium for lossless propagation with nanoscale confinement," *Opt. Lett.* **36**(12), 2312–2314 (2011).
34. Y. S. Bian, Z. Zheng, X. Zhao, L. Liu, Y. L. Su, J. S. Liu, J. S. Zhu, and T. Zhou, "Hybrid plasmon polariton guiding with tight mode confinement in a V-shaped metal-dielectric groove," *J. Opt.* **15**(5), 055011 (2013).
35. G. Veronis and S. H. Fan, "Guided subwavelength plasmonic mode supported by a slot in a thin metal film," *Opt. Lett.* **30**(24), 3359–3361 (2005).

---

## 1. Introduction

The goal of manipulating light at the subwavelength scale has motivated extensive research into a number of waveguiding structures that could support light propagation well beyond the fundamental diffraction limit [1]. Surface plasmon polariton (SPP) based waveguides are promising candidates for subwavelength light guiding due to their capabilities of providing truly nanoscale confinement along two dimensions. Owing to their fascinating optical properties, they have been considered as important building blocks for novel miniaturized photonic components and circuits [2].

Up to date, a number of SPP waveguiding structures have been proposed and investigated, which include metallic nanowires [3], metal stripes embedded in homogeneous dielectrics [4], metal slots [5] or channels [6, 7] cut into metal substrate as well as triangular metal wedges [8]. However, for most of these conventional SPP waveguides, the tradeoff between the mode confinement and transmission loss could not be well balanced. Metal slot waveguide [5] could offer nanoscale confinement of the lightwave but its modal loss is relatively high due to the

significantly increased field strength in the metallic structure. On the other hand, metallic stripe structures could support the propagation of ultra-low-loss plasmonic modes. However, their confinement is weak and the mode size is typically larger than the wavelength scale [4].

Recently, a novel hybrid plasmonic waveguide that leverages the coupling between dielectric and plasmonic modes has demonstrated better capabilities to compromise the propagation loss and field confinement [9]. Through introducing an additional low-index layer between the high-index structure and the metal waveguide, the strong coupling between different optical modes has resulted in a novel hybridized mode featuring strong field localization near the low-index gap with low modal loss. Its nice optical performance has enabled the realization of plasmon nanolasers [10], and also facilitated the operation of numerous ultra-compact passive plasmonic devices [11–15]. Furthermore, a number of modified hybrid structures have also been intensively studied, which include metal-dielectric-slabs [16–20], dielectric-loaded type [21–23], dielectric-rib waveguide [24], coaxial structure [25, 26], nanowire array [27], metal-insulator-metal type [15, 28–31], and wedge [32] or ridge [33] configurations.

Here in this paper, we would like to leverage the guiding capability of a rectangular metallic trench [7]. By combining high-index dielectric with a metal trench structure, a novel hybrid plasmonic waveguide featuring both low propagation loss and strong optical confinement can be realized. In the following section, we will carry out detailed investigations on the properties of the fundamental hybrid plasmonic modes against the changes of key geometric parameters at the telecom wavelength.

## 2. Geometries and modal properties of the hybrid metal trench waveguide

Figure 1 schematically shows the geometry of the proposed hybrid trench waveguide, where a rectangular high-index dielectric core is embedded inside the metal trench, with thin low-index gaps between the core and the sidewalls of the metal trench. The materials of the low-index gaps and the cladding are assumed to be the same. The depth of the metal trench and the height of the dielectric core are denoted as  $T$ . The width of the dielectric core is  $W_d$ . The gap distance between the dielectric core and the sidewall is  $W_s$ . The low-index dielectric layer has a thickness  $T$ . The refractive indices of the metal trench, dielectric core and the cladding are  $n_m$ ,  $n_d$  and  $n_c$ , respectively. The modal properties of the hybrid waveguides are investigated at  $\lambda = 1550$  nm by the finite-element method (FEM) using COMSOL<sup>TM</sup>. Scattering boundary conditions along with extremely fine mesh are applied near the gap regions to ensure accurate solutions. In the simulations, the metal trench is assumed to be silver (Ag) and its refractive index is  $n_m = 0.1453 + 11.3587i$  [27]. The high-index core is first assumed as silicon and has a refractive index of 3.5. In the following studies, the depth of the metal trench (i.e. height of the dielectric core) is set at  $T = 400$  nm without specific notifications.

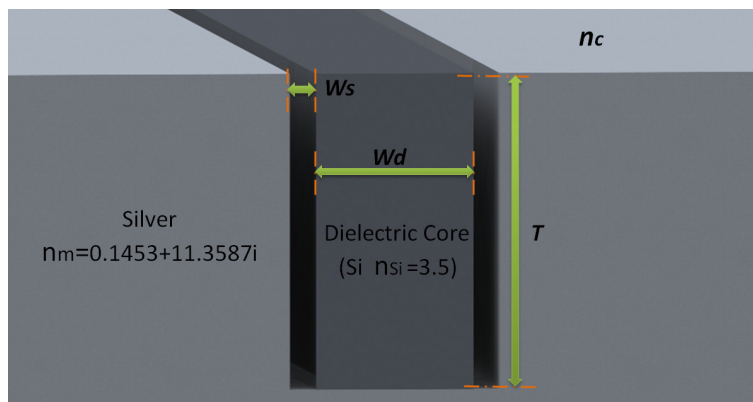


Fig. 1. Schematic illustration of the studied hybrid trench waveguide.

We firstly look into the propagation property of the proposed hybrid trench structure, where the results of the conventional metal trench without the high-index core and the proposed hybrid structure are both shown in Fig. 2. The propagation length is calculated by

$$L = \lambda / [4\pi \text{Im}(N_{eff})] \quad (1)$$

Here,  $\text{Im}(N_{eff})$  is the imaginary part of the modal effective index. It can be seen from the figure that, the propagation lengths for both cases would reduce monotonically with the increase of the refractive index of the cladding. Figure 2 also illustrates that, compared to the conventional metal trench, the proposed hybrid trench has lower modal loss, and its propagation length can be more than 2 times larger than the conventional one. For instance, as show in the figure, for  $W_s = 25 \text{ nm}$  and  $W_s = 50 \text{ nm}$ , when  $n_c = 1$ , the propagation length are  $15 \mu\text{m}$  and  $25 \mu\text{m}$  for conventional metal trench waveguide, and are  $55 \mu\text{m}$  and  $60 \mu\text{m}$  for our proposed hybrid structure. On the other hand, when  $n_c = 3$ , the propagation lengths of the conventional metal trench and hybrid trench are  $5 \mu\text{m}$  and  $20 \mu\text{m}$  for  $W_s = 25 \text{ nm}$ , and  $8 \mu\text{m}$  and  $22 \mu\text{m}$  for  $W_s = 50 \text{ nm}$ , respectively.

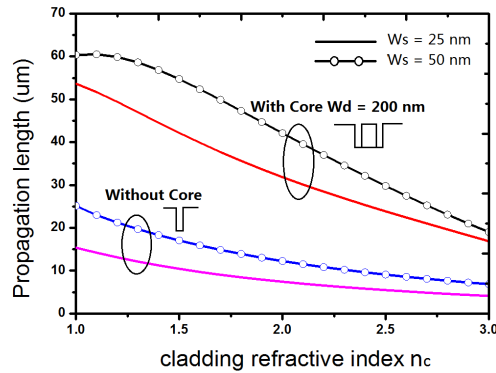


Fig. 2. Dependence of the propagation lengths of the conventional metal trench and hybrid trench waveguides on the refractive index of the cladding layer.

To explain the difference between the modal losses of the two structures, we further show the profiles of the two plasmonic modes. In Fig. 3, the energy density distributions of the conventional metal trench structure and the proposed hybrid trench waveguide are depicted. It is clearly illustrated that, for the proposed hybrid waveguide, a large portion of the modal energy can be confined in the dielectric core, thereby resulting in lower propagation loss. However, for the conventional metal trench waveguide, due to the strong confinement in the metal, its modal loss is much larger than the hybrid case.

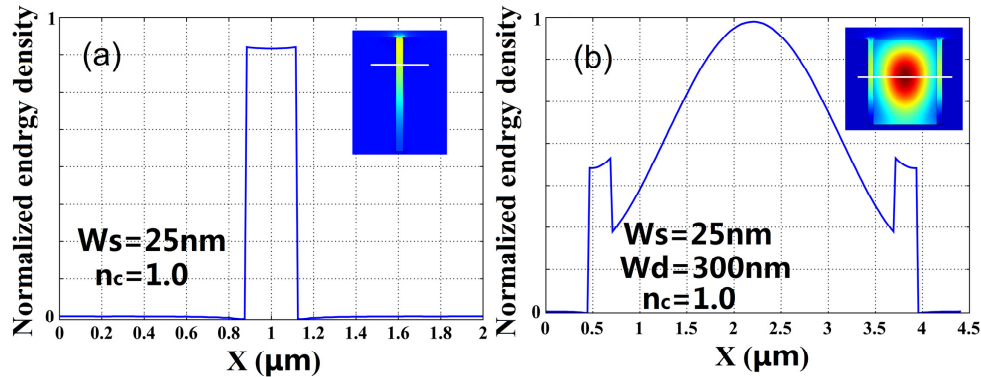


Fig. 3. Normalized energy density distributions of (a) conventional metal trench waveguide; (b) hybrid trench waveguide.

We then investigate the propagation properties of the hybrid trench mode for structures with dielectric cores of different size. Here the transmission loss can be calculated by the following equation [10], and the calculated results of the propagation length and the transmission loss are shown in Fig. 4(a) and 4(b), respectively.

$$\alpha = -\frac{40\pi \text{Im}(n_{\text{eff}})}{\lambda} \log e \quad (2)$$

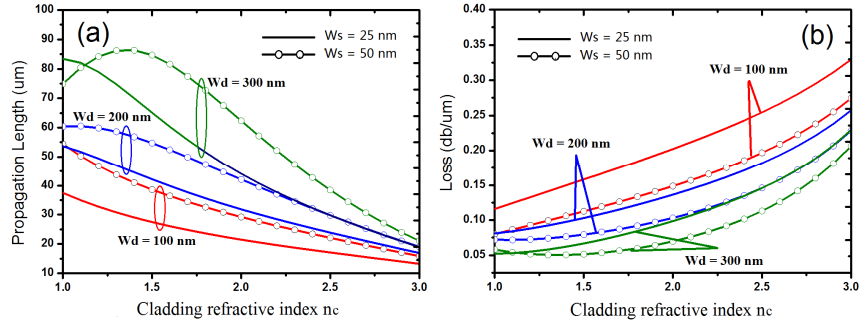


Fig. 4. Propagation properties for waveguides with different dielectric core sizes and claddings: (a) propagation length and (b) transmission loss.

It can be seen from Fig. 4 that, for small  $W_d$  and small gap width, increasing the refractive index of the cladding would lead to the monotonic decrease of the propagation length and increase in the transmission loss. However, when both the dielectric core and the gap width are relatively large (e.g.  $W_d = 300$  nm,  $W_s = 50$  nm or  $W_d = 200$  nm,  $W_s = 50$  nm), the changes of the propagation properties demonstrate non-monotonic trends.

In order to explain the above phenomenon more clearly, we need to elaborate the basic working principle of our waveguide. The coupling between the dielectric mode and plasmonic mode plays an important role in determining the modal characteristics. Owing to the presence of the high-index dielectric core, the energy that originally concentrated in two independent slit waveguide gets strongly coupled in the dielectric core. Two physical parameters including the refractive index of cladding material and the size of the high-index core (core width) will significantly influence the coupling efficiency. Therefore, when the refractive index of the cladding material changes, the hybrid mode would demonstrate quite different properties. Figure 5 shows the energy density distributions of a typical hybrid trench structure with  $W_d = 300$  nm and  $W_s = 50$  nm. It is clear seen that, due to the high refractive index contrast and the relatively large dielectric core size, most of the mode energy can be stored inside the dielectric core when the refractive index of the cladding is small (e.g. see the results of  $n_c = 1$  and  $n_c = 1.5$ ). As the cladding's refractive index continuously gets larger, more energy would be released from the dielectric core into the low-index gap and the metal region (e.g. see  $n_c = 2$ ). Finally, when  $n_c$  gets very large (approaching  $n_d$ , i.e. 3.5), a large portion of the mode energy will be located around the sharp corners of the metal trench, leading to an increased modal loss.

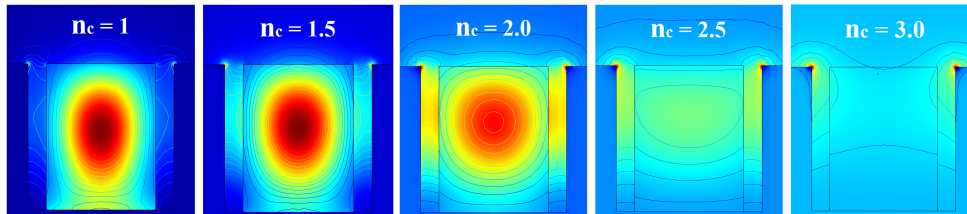


Fig. 5. Energy density distribution of the hybrid trench waveguide ( $W_d = 300$  nm,  $W_s = 50$  nm) with different cladding material.

The confinement factor, defined as the power ratio inside each element to the total power of the waveguide, is a widely employed parameter to evaluate the confinement capability of the waveguide. In Fig. 6 we show the dependence of the confinement factor on  $n_c$  for various core size. It is illustrated that, for configurations with relatively large dielectric cores, a large portion of the mode energy can be resided in the dielectric core when  $n_c$  is small, which is consistent with the energy distributions shown in Fig. 5. This energy ratio would decrease monotonically when  $n_c$  gradually increases, as also can be seen from the distributions in Fig. 5. On the other hand, when the dielectric core size is relatively small (e.g.  $W_d = 100$  nm), the energy inside the core is quite limited, and it demonstrate non-monotonic trends with the changing of the cladding's refractive index, which indicates the existence of an optimized  $n_c$  regarding the energy confined inside the dielectric core.

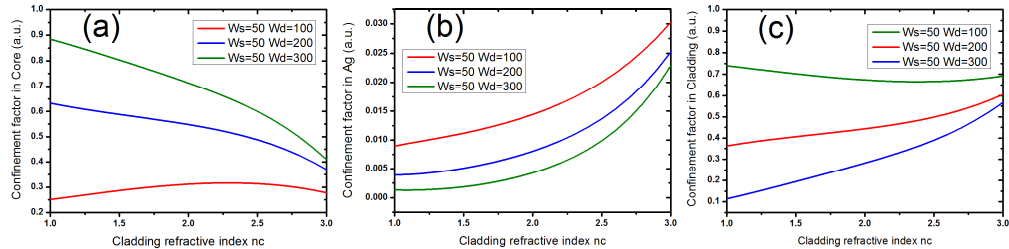


Fig. 6. The effect of the cladding layer's refractive index on the confinement factor for waveguides with different geometries: (a) confinement factor in the dielectric core; (b) confinement factor in the Ag trench; (c) confinement factor in the cladding and the gap region.

Figure 7 shows the relationship between the imaginary part of the modal effective index and the core width. Because the propagation length inversely proportional to the imaginary part of the waveguide's modal effective index, point A and point B show two critical values for  $W_d$ . Considering  $W_s = 50$  nm, when  $W_d > A$ , the propagation length is decreasing monotonically with the increasing of the cladding's refractive index. On the other hand, when  $W_d < A$ , the propagation length will increase first before it decreases with the increasing of  $n_c$ . It is also noted from Fig. 7 that, when  $W_d < B$ , the propagation length of  $W_s = 50$  nm waveguide will always larger than that of  $W_s = 25$  nm.

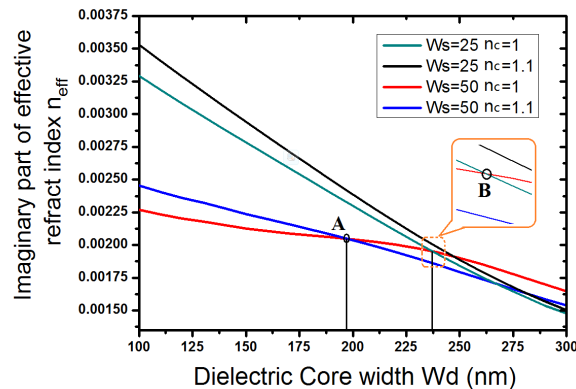


Fig. 7. Relationship between the imaginary part of modal effective index and the core width.

Finally, we show the dependence of propagation length and transmission loss on the height of the dielectric core. It is clearly seen in Fig. 8 that, increasing the height of the dielectric core could lead to the monotonic increase of the modal loss and thus decrease in the propagation length. It is noted that, within the considered physical dimensions, low modal loss could be readily achieved, indicating reasonable propagation lengths for practical applications.

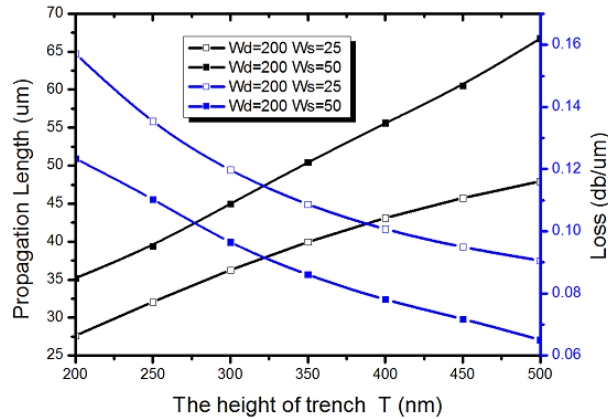


Fig. 8. Dependence of propagation length of the hybrid mode on the height of the trench (dielectric core).

The above discussions clearly reveal the nice optical performance of the proposed structure at the telecom wavelength. Compared to the metallic V-groove structure, the hybrid metal trench waveguide could realize much tighter confinement of light owing to the strong hybridization between the dielectric and plasmonic modes [31, 34]. On the other hand, the proposed hybrid waveguide enables much lower propagation loss than the standard metal slot waveguide [35], while maintaining subwavelength mode size. Here, it is also worth mentioning that, considering the practical fabrication processes, the proposed hybrid waveguide could have non-vertical metallic sidewalls (i.e. trapezoidal shaped metal trench). It is shown that similar modal behaviors can be obtained for these modified hybrid trench waveguides, and their propagation losses can be even smaller than the rectangular-type structures studied here.

### 3. Conclusions

In summary, we have proposed and investigated a novel plasmonic waveguide that comprises a high-index dielectric core embedded inside a rectangular-shaped metallic trench structure. Numerical simulations reveal that the dielectric core can concentrate a large portion of the mode energy and also greatly reduce the propagation loss of the traditional metal trench waveguide. Through optimization of the dielectric core size and the refractive index of the cladding material, long propagation distance with strong optical confinement could be achieved simultaneously at the telecom wavelength. The studied hybrid structure could be employed to build highly efficient passive devices and may find other interesting applications as well.

### Acknowledgments

This work was supported by MOST Grants (No. 2009CB930700), NSFC Grants (Nos. 11004237, 11134013, 11227407) and “Knowledge Innovation Project” (KJCX2-EW-W04) of CAS.